2021 43rd Annual International Conference of the
IEEE Engineering in Medicine & Biology Society (EMBC)
Oct 31 - Nov 4, 2021. Virtual Conference

An ICA Investigation into the Effect of Physiological Noise Correction on Dimensionality and Spatial Maps of Intrinsic Connectivity Networks

Behnaz Jarrahi, *Member, IEEE*

***Abstract*— Physiological processes such as cardiac pulsations and respiration can induce signal modulations in functional magnetic resonance imaging (fMRI) time series, and confound inferences made about neural processing from analyses of the blood oxygenation level-dependent (BOLD) signals. Retrospective image space correction of physiological noise (RETROICOR) is a widely used approach to reduce physiological signals in data. Independent component analysis (ICA) is a valuable blind source separation method for analyzing brain networks, referred to as intrinsic connectivity networks (ICNs). Previously, we showed that temporal properties of the ICA-derived networks such as spectral power and functional network connectivity could be impacted by RETROICOR corrections. The goal of this study is to investigate the effect of retrospective correction of physiological artifacts on the ICA dimensionality (model order) and intensities of ICN spatial maps. To this aim, brain BOLD fMRI, heartbeat, and respiration were measured in 22 healthy subjects during resting state. ICA dimensionality was estimated using minimum description length (MDL) based on i.i.d. data samples and smoothness FWHM kernel, and entropy-rate based order selection by finite memory length model (ER-FM) and autoregressive model (ER-AR). Differences in spatial maps between the raw and denoised data were compared using the paired t-test and false discovery rate (FDR) thresholding was used to correct for multiple comparisons. Results showed that ICA dimensionality was greater in the raw data compared to the denoised data. Significant differences were found in the intensities of spatial maps for three ICNs: basal ganglia, precuneus, and frontal network. These preliminary results indicate that the retrospective physiological noise correction can induce change in the resting state spatial map intensity related to the within-network connectivity. More research is needed to understand this effect.**

I. INTRODUCTION

One of the challenges in inferring meaningful information related to neuronal activity from the blood oxygen level-dependent functional magnetic resonance imaging (BOLD fMRI) has been the presence of physiological signals in fMRI [1]. These signals originate predominantly from the cardiorespiratory system and they are capable of modifying BOLD signals by, e.g., inducing changes in the magnetic field (B0) due to respiration induced chest movement, or the pulsatility of cerebrospinal fluid during each heartbeat [2]. One of the methods that has been proposed to reduce the effect of physiological signals in fMRI data is retrospective correction in imaging space (RETROICOR; [1]). RETROICOR uses a low-order Fourier transform, and includes measures of cardiorespiratory phases in a regression model which is applied to each voxel's data separately [1].

B. Jarrahi is with the Department of Anesthesia, Stanford University, CA, USA; (email: behnaz.jarrahi@stanford.edu).

Blind source separation techniques such as independent component analysis (ICA) can recover a set of signals from their linear mixtures, and has been shown to be capable of separating out different sources of signals including physiological noise in fMRI data. ICA can decompose fMRI data into a set of maximally independent maps in the spatial or temporal domain [3]. Spatial ICA methods can decompose fMRI data into functional brain networks, which are often referred to as intrinsic connectivity networks (ICNs). These networks show consistent, though not identical, spatial patterns in the absence or presence of task. Understanding the variability of these networks in clinical settings has become increasingly important especially in biomarker studies.

Previously, we showed that RETROICOR corrections induce changes in the ICN temporal properties, namely power spectra and functional network connectivity [4]. In this study we aim to examine the effect of physiological denoising on ICA dimensionality (model order), i.e., estimation of the number of informative components in the data, and spatial map intensities related to the degree of connectivity and coactivation within a network. We use the minimum description length (MDL), and entropy-rate (ER) order selection algorithms to estimate the number of independent source components. Following the statistical framework proposed in [3], we will perform ICA decomposition at relatively high model order of 75 and measure the reliability of decomposition by ICASSO [5]. Finally, we evaluate resultant ICN spatial map intensities to identify the effects of RETROICOR corrections throughout cortical and subcortical networks.

II. MATERIALS AND METHODS

A. Data Acquisition

Resting state fMRI data was collected from 22 healthy volunteers (12 females; mean age: 37.73 ± 11.32 years). All subjects provided written, IRB-approved consent and were compensated. During the scan, they were asked to stay still and relax with their eyes closed but avoid falling into sleep. Scans were acquired on a 3.0 T GE scanner using EFGRE3D pulse sequence with 2.0-s repeat time, 30-ms echo time, 22-cm field of view, 64×64 acquisition matrix, 76^o flip angle, 4-mm slice thickness, 1-mm gap, 31 slices, and ascending acquisition. 360 volumes were acquired per scan. Subjects' heart beats were recorded using a pulse-oximeter and respiration was measured with a plethysmograph. General exclusion criteria included a history of head injury, neurological disorders, or MRI incompatibility such as having mental implants or pregnancy.

978-1-7281-1178-0/21/$31.00 ©2021 IEEE

B. Data Preprocessing

Upon completion of scans, two copies of the dataset were created. One copy underwent RETROICOR correction [1] (denoised), while the other did not (raw). All images were preprocessed using Statistical Parametric Mapping version 12b (SPM12b, Wellcome Department of Cognitive Neurology). Preprocessing of resting state functional images involved motion correction using rigid body transformation, slice time correction, spatial normalization to MNI space, spatial smoothing with a Gaussian kernel of FWHM of 8 mm and intensity normalization [3].

C. Model Order Estimation

We used different methods for estimating the number of independent source components:

1) The MDL criterion is based on model selection formulation by Wax and Kailath. This algorithm implements information theoretic criterion and down-samples the data to obtain independent and identically distributed (i.i.d.) samples [6].
2) The MDL criterion based on full width at half maximum (FWHM). This method skips i.i.d sampling of the datasets [6]. 5 mm smoothness FWHM kernel was used.
3) Entropy-rate based order selection by finite memory length model (ER-FM). This algorithm estimates the ICA model order for dependent samples by considering all the samples to estimate the likelihood. The likelihood estimators assume the signal to have finite memory length [7].
4) Entropy-rate based order selection by autoregressive model (ER-AR). Similar to ER-FM, this algorithm also estimates the order for dependent samples from all the samples to estimate the likelihood. However, the likelihood estimators assume that the signals can be modeled by an autoregressive mode [7].

D. Group independent components analysis

Group ICA was performed using the Group ICA of fMRI Toolbox (GIFTv3.0c; University of New Mexico, USA). Following the statistical framework proposed in [3], we chose relatively high model order ICA (number of components = 75) as such high model order can yield more refined components. In the first step, subject-specific data reduction principal component analysis (PCA) was performed, which resulted in retaining 100 PCs with a standard economy-size decomposition. In the second step, group data reduction resulted in retaining 75 PCs using the expectation-maximization algorithm. The Infomax ICA algorithm was repeated 20 times in ICASSO to estimate the reliability of the decomposition [5]. The quality of component clusters was quantified using the Iq index. Iq is a number between 0 to 1 and reflects the difference between intra-cluster and extra-cluster similarity [3], [5]. In the third and final step, subject-specific spatial maps and their corresponding time courses were estimated using the GICA3 back-reconstruction method in GIFT software.

We identified a subset of components considered to be ICNs using the procedures described in our earlier works [4], [8]–[10]. Briefly, components with $Iq < 0.8$ was eliminated. Artifactual components were also discarded upon visual inspection based on their motion-related spatial maps, peak activation in the ventricles, or domination of their time courses by high frequency power [3]. To facilitate evaluation, multiple spatial regression analysis were also performed on the components with publicly available network templates [3]. For the set of selected ICNs, component spatial maps were thresholded to focus the analysis on the voxels that were most representative of each network. To define significant brain regions associated with each ICN, back-reconstructed spatial maps was normalized into z scores, and the averaged maps of z scores were entered into second-level random effects analysis in SPM12. The significance threshold was set at family-wise error (FEW)-corrected threshold of $p < 0.05$ for multiple comparisons of voxel-wise whole-brain analysis. The highest t-value and the locus of the peak activation (x, y, z) in MNI coordinates were saved. Differences in spatial maps between the raw and denoised data were compared using the paired t-test with the mancovan toolbox in GIFT package. False discovery rate (FDR) thresholding was used to correct for multiple comparisons at $p < 0.05$.

III. RESULTS

Table 1. Estimated Independent Components	Mean	Median	Std	Min	Max
Method 1: MDL (i.i.d. Sampling)					
Raw	71	71	73	10.04	54	90
Denoised	68	68.36	69.5	10.23	48	87
Method 2: MDL (FWHM)					
Raw	41	41.36	43	5.42	31	49
Denoised	37	37.23	39	5.84	24	45
Method 3: ER-FM					
Raw	207	206.68	207	27.27	150	248
Denoised	206	205.91	207	26.27	152	247
Method 4: ER-AR					
Raw	205	204.77	205.5	27.18	149	248
Denoised	203	203.14	204	26.36	149	246

Results of model order estimation are summarized in Table 1. All 22 subjects were used for ICA model order estimation and separately for each condition. Mean, median, max and standard deviation are reported.

From 75-IC decomposition, thirty-six components were identified as ICNs (Fig. 1). They are grouped by their anatomical and functional properties into the precuneus (PN), visual (VN), sensorimotor (SMN), auditory (AUD), default-mode (DMN), language (LN), cognitive/attention (CAN), sub-cortical (SCN), and cerebellar (CBN) networks. The resultant ICNs are very similar to those found in previous studies with high model order ICA [3]. The quality index (Iq) associated with each ICN, number of voxels at FWE-corrected p-value; maximum t-statistic (tmax); peak coordinate (in mm) of tmax in MNI space are displayed in Table 2. Paired t-test results for raw – denoissed datasets are shown at uncorrected $p < 0.05$ (Fig. 2A), and FDR-corrected $p < 0.05$ (Fig. 2B). The ICNs that survived FDR-correction are displayed separately in Fig. 2C.

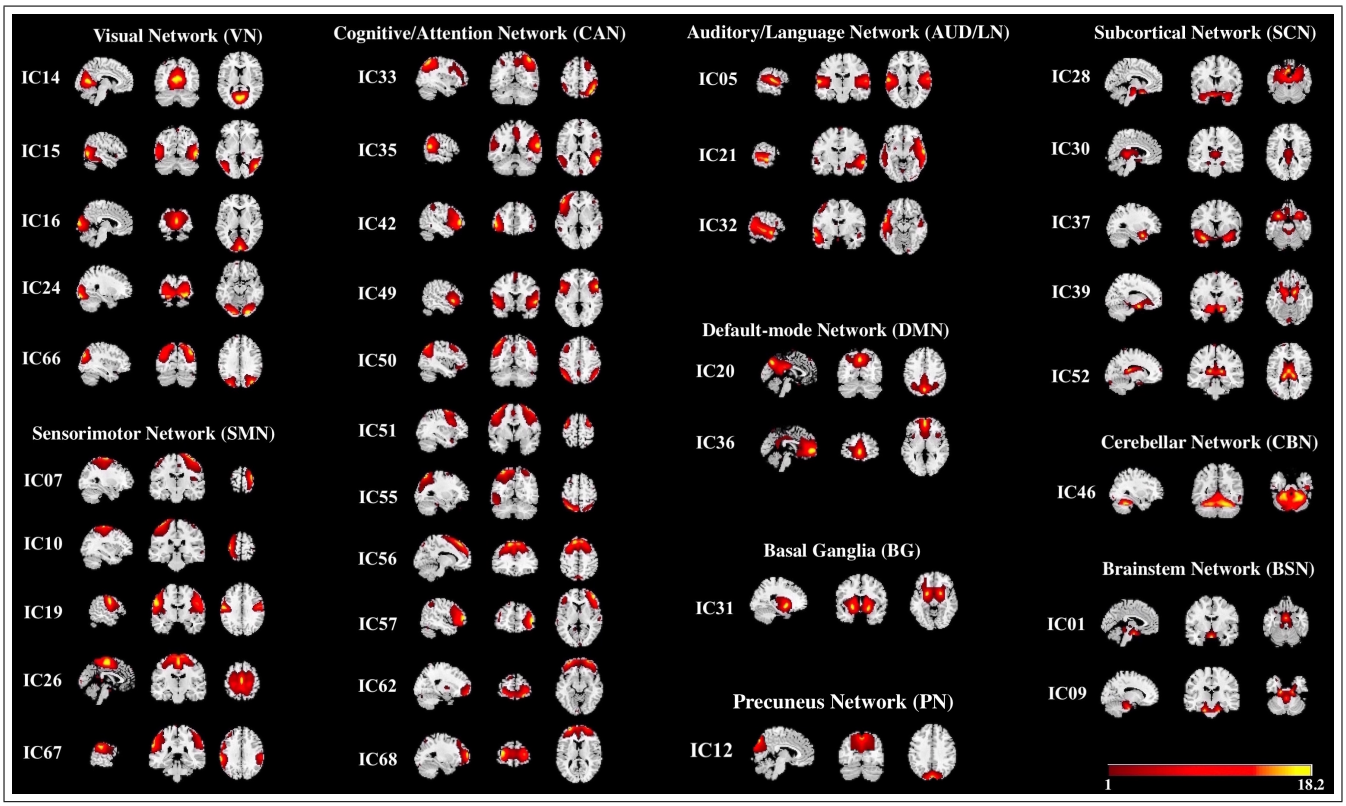

Fig. 1. Spatial maps of 36 ICNs shown in neurological convention (right is right), FEW-corrected $p < 0.05$.

Table 2. ICN Spatial Map Parameters

ICN	IC#	IQ	Raw						Denoised					
			Vol (vox)	Tmax	x	y	z	Peak	Vol (vox)	Tmax	x	y	z	Peak
PN	IC12	0.979	4935	21.06	-12	-90	18	L Superior Occipital Gyrus	5066	21.1	2	-90	20	L Cuneus
VN	IC14	0.979	8444	26.83	-2	-78	0	R Lingual Gyrus	8427	27.1	-2	-78	0	L Lingual Gyrus
	IC15	0.981	7648	18.09	-50	-74	6	L Middle Occipital Gyrus	7652	19.07	44	-78	-2	R Inferior Occipital Gyrus
	IC16	0.980	5101	18.71	0	-90	-8	L Calcarine Gyrus	5094	19.33	0	-90	-10	L Calcarine Gyrus
	IC24	0.974	5273	24.11	26	-96	-8	R Inferior Occipital Gyrus	5276	25.07	26	-96	-8	R Inferior Occipital Gyrus
	IC66	0.926	9705	25.9	42	-80	28	R Middle Occipital Gyrus	9461	25.44	42	-80	28	R Middle Occipital Gyrus
SMN	IC07	0.980	5797	20.06	48	-18	46	R Precentral Gyrus	5746	20.21	48	-16	44	R Precentral Gyrus
	IC10	0.978	5531	16.81	-34	-6	70	L Postcentral Gyrus	5611	20.54	-42	-36	66	L Postcentral Gyrus
	IC19	0.979	5408	15.89	-60	-2	16	L Postcentral Gyrus	5607	17.73	-62	-2	16	L Postcentral Gyrus
	IC26	0.976	15899	30.11	0	-4	56	L Posterior-Medial Frontal	15780	27.46	-18	-40	66	L Postcentral Gyrus
	IC67	0.834	9246	23.62	-58	-26	26	L SupraMarginal Gyrus	9270	22.23	-58	-28	28	L SupraMarginal Gyrus
AUD	IC05	0.978	11975	26.97	-38	-28	12	L Heschls Gyrus	11973	24.98	-38	-28	12	L Heschls Gyrus
DMN	IC20	0.978	7036	21.13	0	-60	28	L Precuneus	7050	21.79	0	-60	28	L Precuneus
	IC36	0.970	11522	32.73	-10	38	-12	L Mid Orbital Gyrus	11121	34.03	0	34	-12	R Mid Orbital Gyrus
CAN	IC21	0.979	7938	18.69	54	-22	-10	R Middle Temporal Gyrus	8040	22.42	60	2	-20	R Middle Temporal Gyrus
	IC32	0.976	10794	22.67	-44	10	-24	L Temporal Pole	11067	21.59	-44	10	-26	L Medial Temporal Pole
	IC33	0.975	8487	25.33	38	-48	48	R Inferior Parietal Lobule	8808	26.34	38	-48	48	R Inferior Parietal Lobule
	IC35	0.975	8778	32.29	58	-56	16	R Middle Temporal Gyrus	8535	38.26	58	-56	16	R Middle Temporal Gyrus
	IC42	0.967	9260	25.15	-46	40	-8	L IFG (p. Orbitalis)	8831	27.68	-46	40	-8	L IFG (p. Orbitalis)
	IC49	0.968	7746	22.08	40	16	-10	R Insula Lobe	7689	20.72	40	16	-10	R Insula Lobe
	IC50	0.966	7700	27	50	-58	32	R Angular Gyrus	7575	25.36	-42	-54	40	L Inferior Parietal Lobule
	IC51	0.952	11370	25.34	50	18	32	R IFG (p. Opercularis)	11443	24.26	52	18	32	R IFG (p. Opercularis)
	IC55	0.959	7057	23.38	-28	-64	42	L Inferior Parietal Lobule	6825	19.98	-38	-66	52	L Superior Parietal Lobule
	IC56	0.943	15935	26.49	-10	44	34	L Superior Medial Gyrus	15973	28.34	-10	46	30	L Superior Medial Gyrus
	IC57	0.937	5910	20.77	44	14	20	R IFG (p. Triangularis)	5832	18.8	44	34	6	R IFG (p. Triangularis)
	IC62	0.898	4796	23.31	28	56	-16	R Middle Orbital Gyrus	4768	22.08	28	58	-16	R Middle Orbital Gyrus
	IC68	0.854	8356	21.51	-20	62	6	L Superior Frontal Gyrus	8256	23.46	-24	50	10	L Middle Frontal Gyrus
BG	IC31	0.977	11746	20.99	-10	10	-6	L Putamen	12207	18.58	-8	10	-4	L Caudate Nucleus
SCN	IC28	0.975	7686	23.25	-24	-10	-22	L Hippocampus	7288	21.25	-26	-8	-22	L Hippocampus
	IC30	0.979	4186	21.33	-8	-28	8	L Thalamus	4386	22.25	-8	-28	8	L Thalamus
	IC37	0.974	5998	18.51	-34	-12	-16	L Hippocampus	5989	18.43	-34	12	-22	L Temporal Pole
	IC39	0.968	2177	14.48	-24	-4	-20	L Amygdala	1995	14.58	-24	-2	-20	L Amygdala
	IC52	0.968	3857	14.86	-2	-10	12	L Thalamus	3628	15.1	-2	-24	8	L Thalamus
CBN	IC46	0.973	10015	31	16	-50	-20	R Cerebelum (IV-V)	9769	29.9	16	-50	-20	R Cerebelum (IV-V)
BSN	IC01	0.986	1258	20.69	6	-14	-30	R Brainstem	1413	20.77	6	-14	-30	R Brainstem
	IC09	0.980	1976	15.78	-8	-40	-34	L Brainstem	2053	15.88	-8	-40	-34	L Brainstem

IV. Conclusion

Considering the growing interest in ICA network analysis, the goal of this study was to determine if physiological noise correction impacts ICA model order and spatial map intensities. Results revealed that ICA dimensionality was lower for data with RETROICOR correction. In addition, significant changes were observed in spatial maps with RETROICOR correction. Decrease in spatial map intensities was particularly pronounced (FDR-corrected $p < 0.05$) in basal ganglia (IC 31), precuneus (IC 12), and frontal networks (IC 62) (Fig. 2B). ICN spatial map intensities can be considered a measure of within-network connectivity strength. Denoising reduced the cohesiveness and intra-network connectivity in the above-mentioned networks. We also observed coordinates of peak voxel shifted from putamen to caudate nucleus in the basal ganglia network, and from superior occipital gyrus to cuneus in precuneus network with RETROICOR (Table 2). On the basis of these preliminary results, removal of such physiological signals from BOLD data must be carefully evaluated as these signals might not be noise per se, but a theoretically meaningful component of the signal to investigate brain function [11].

References

[1] G. H. Glover, T.-Q. Li, and D. Ress, "Image-based method for retrospective correction of physiological motion effects in fmri: Retroicor," *Magnetic Resonance in Medicine: An Official Journal of the International Society for Magnetic Resonance in Medicine*, vol. 44, no. 1, pp. 162–167, 2000.

[2] T. T. Liu, "Noise contributions to the fmri signal: An overview," *NeuroImage*, vol. 143, pp. 141–151, 2016.

[3] E. A. Allen, E. B. Erhardt, Damaraju, *et al.*, "A baseline for the multivariate comparison of resting-state networks," *Frontiers in systems neuroscience*, vol. 5, 2011.

[4] B. Jarrahi and S. Mackey, "Measuring the influence of physiological noise corrections on ica derived intrinsic connectivity brain networks in rest and task fmri," in *2018 40th Annual International Conference*

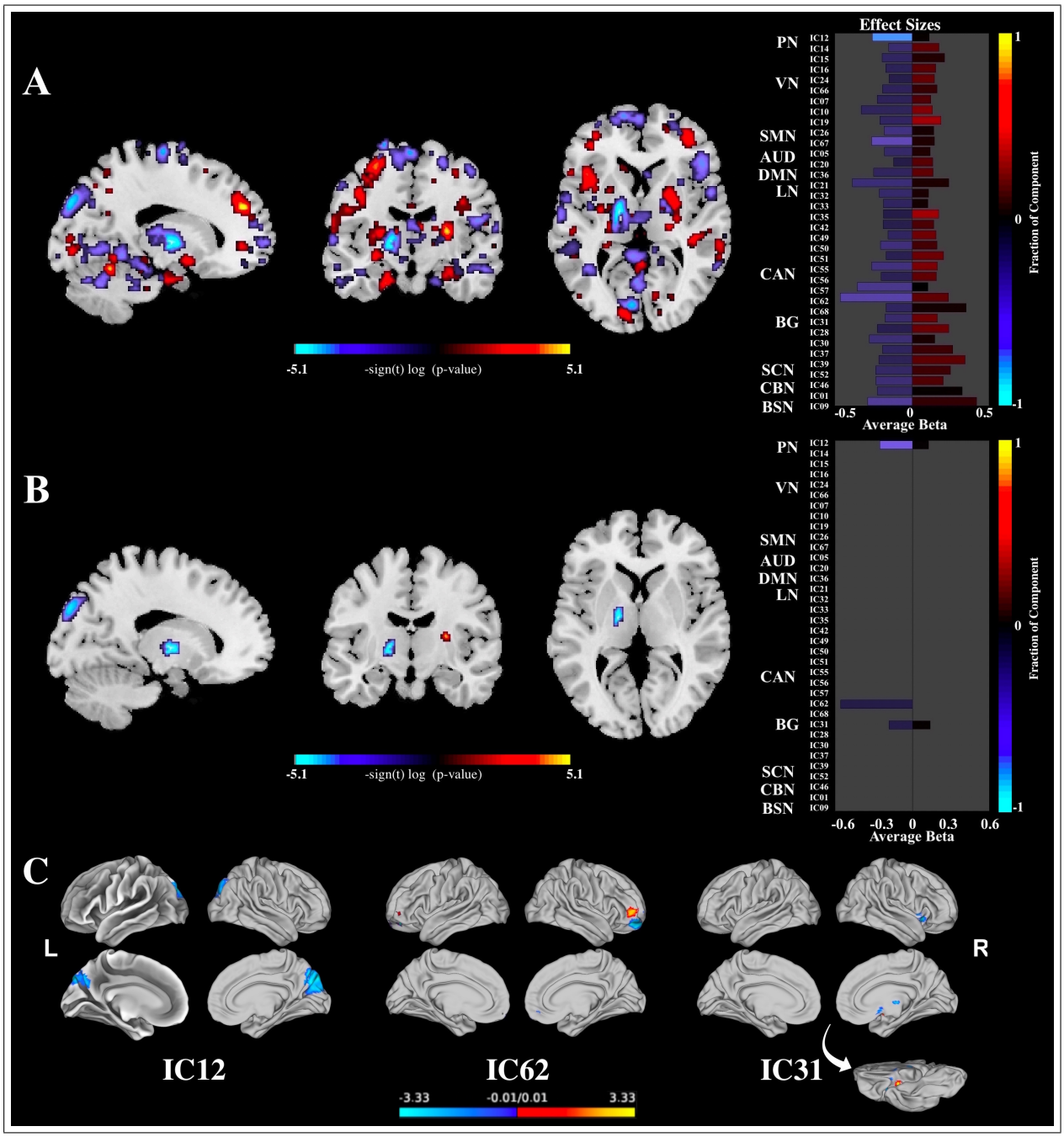

Fig. 2. Paired t-test results showing the effects of retrospective physiological noise correction on spatial maps at **A** uncorrected $p < 0.05$, and **B** FDR-corrected $p < 0.05$. Right panels show bar plots of the average beta-values. **C** Individual components with significant RETROICOR correction effects.

of the IEEE Engineering in Medicine and Biology Society (EMBC). IEEE, 2018, pp. 1046–1049.

[5] J. Himberg and A. Hyvarinen, "Icasso: software for investigating the reliability of ica estimates by clustering and visualization," in *2003 IEEE XIII Workshop on Neural Networks for Signal Processing (IEEE Cat. No. 03TH8718)*. IEEE, 2003, pp. 259–268.

[6] Y.-O. Li, T. Adalı, and V. D. Calhoun, "Estimating the number of independent components for functional magnetic resonance imaging data," *Human brain mapping*, vol. 28, no. 11, pp. 1251–1266, 2007.

[7] G.-S. Fu, M. Anderson, and T. Adalı, "Likelihood estimators for dependent samples and their application to order detection," *IEEE transactions on signal processing*, vol. 62, no. 16, pp. 4237–4244, 2014.

[8] B. Jarrahi and D. Mantini, "The nature of the task influences intrinsic connectivity networks: An exploratory fmri study in healthy subjects," in *2019 9th International IEEE/EMBS Conference on Neural Engineering (NER)*. IEEE, 2019, pp. 489–493.

[9] B. Jarrahi and S. Kollias, "Impact of intravesical cold sensation on functional network connectivity estimated using ica at rest & during interoceptive task," in *2020 42nd Annual International Conference of the IEEE Engineering in Medicine & Biology Society (EMBC)*. IEEE, 2020, pp. 1722–1725.

[10] B. Jarrahi and S. Mackey, "Characterizing the effects of mr image quality metrics on intrinsic connectivity brain networks: A multivariate approach," in *2018 40th Annual International Conference of the IEEE Engineering in Medicine and Biology Society (EMBC)*. IEEE, 2018, pp. 1041–1045.

[11] V. Iacovella and U. Hasson, "The relationship between bold signal and autonomic nervous system functions: implications for processing of "physiological noise"," *Magnetic resonance imaging*, vol. 29, no. 10, pp. 1338–1345, 2011.